

# ARM: A Learnable, Plug-and-Play Module for CLIP-based Open-vocabulary Semantic Segmentation

Ziquan Liu Zhewei Zhu

Xuyang Shi\*

Southwest University of Science and Technology, China

{ziquanliu, zhuzhewei, xuyangshi}@mails.swust.edu.cn

January 1, 2026

## Abstract

Open-vocabulary semantic segmentation (OVSS) is fundamentally hampered by the coarse, image-level representations of CLIP, which lack precise pixel-level details. Existing training-free methods attempt to resolve this by either importing priors from costly external foundation models (e.g., SAM, DINO) or by applying static, hand-crafted heuristics to CLIP’s internal features. These approaches are either computationally expensive or sub-optimal. We propose the Attention Refinement Module (ARM), a lightweight, learnable module that effectively unlocks and refines CLIP’s internal potential. Unlike static-fusion methods, ARM learns to adaptively fuse hierarchical features. It employs a semantically-guided cross-attention block, using robust deep features ( $K, V$ ) to select and refine detail-rich shallow features ( $Q$ ), followed by a self-attention block. The key innovation lies in a “train once, use anywhere” paradigm. Trained once on a general-purpose dataset (e.g., COCO-Stuff), ARM acts as a universal plug-and-play post-processor for diverse training-free frameworks. Extensive experiments show that ARM consistently boosts baseline performance on multiple benchmarks with negligible inference overhead, establishing an efficient and effective paradigm for training-free OVSS.

## 1 Introduction

Semantic segmentation is a fundamental task in computer vision that aims to assign a precise category label to each pixel in an image. With the rise of vision-language models (VLMs), particularly CLIP [1], this field has undergone significant transformation. In recent years, numerous studies have focused on applying CLIP to semantic segmentation tasks, leveraging its powerful zero-shot reasoning capability to generalize to categories unseen during training, thereby achieving open-vocabulary semantic segmentation.

However, directly leveraging CLIP for segmentation faces

inherent limitations [2, 3]. CLIP’s pre-training objective maximizes global feature alignment, lacking explicit constraints on pixel-level local consistency. This leads to the patch-level affinity maps produced by its vision encoder being spatially coarse [1, 4, 5], which directly manifests as prevalent artifacts in segmentation results, such as blurry boundaries, loss of fine-grained details, and background noise.

To overcome this challenge, existing research has primarily evolved along two technical routes: training-based methods [6, 7, 8, 9, 10] and training-free methods [11, 5, 12, 13, 14, 15, 4]. The former attempts to fine-tune CLIP on segmentation datasets, but this incurs substantial computational costs and risks sacrificing CLIP’s inherent zero-shot generalization ability [2]. Consequently, training-free methods have become a research focus, endeavoring to adapt CLIP’s pre-trained representations without any additional training.

Training-free methods primarily follow two paradigms. The first, as illustrated in Figure 1(a), relies on external Vision Foundation Models (VFs). These methods [13, 14, 15, 16, 17] introduce high-quality feature priors from other large-scale models [18, 19, 20, 21] to correct and sharpen CLIP’s coarse output. Despite their effectiveness, this approach significantly increases system complexity and computational overhead.

The second, arguably more elegant paradigm focuses on mining CLIP’s internal potential. This line of work can be further categorized: (1) *Final-Layer Attention Modification*: These works [11, 12, 5] observed the spatial invariance of attention maps in CLIP’s final layers and proposed heuristic, training-free modifications to improve localization. (2) *Static fusion of internal cues*: Represented by ResCLIP [4] as shown in Figure 1(b), these methods recognize that intermediate-layer attention maps retain richer spatial details. They aggregate these intermediate maps via a static, hand-crafted strategy and use them as a residual signal to correct the final coarse attention map.

Despite progress in mining CLIP’s internal potential, existing strategies remain sub-optimal. Attention modification methods [11, 12] rely on intricate, hand-crafted heuristic designs. Concurrently, ResCLIP [4] has shown that fusing

\*Corresponding author.

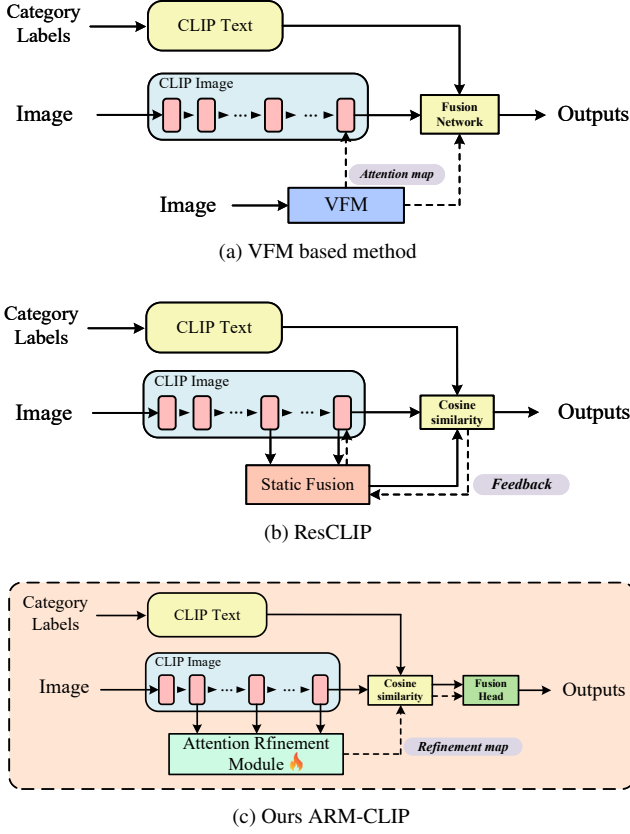


Figure 1: Comparison of different approaches for training-free OVSS. (a) Methods relying on external Vision Foundation Models (VFs) like SAM or DINO. (b) ResCLIP statically fuses intermediate attention maps. (c) Our ARM-CLIP learns to refine CLIP’s hierarchical features using a lightweight trainable module.

intermediate attention maps can effectively improve segmentation performance. However, its static, hand-crafted fusion strategy is non-adaptive and underutilized the rich information available.

This leads to our core question: *If a static fusion of attention maps is already beneficial, can we design a lightweight, learnable module that adaptively leverages CLIP’s hierarchical features to achieve a far superior self-correction?*

Unlike training a task-specific decoder, our approach learns a universal spatial refinement without compromising CLIP’s open-vocabulary capability. To address this, we propose the Attention Refinement Module (ARM), as shown in Figure 1(c). The fundamental difference from ResCLIP is that ARM does not rely on static fusion of attention maps; instead, it learns to adaptively refine hierarchical features. As demonstrated in previous work [19, 22, 23], the ViT model constructs a rich feature hierarchy: shallow layers preserve fine-grained spatial details, such as contours and textures, while deeper layers capture abstract semantic information. Specifically,

ARM extracts shallow/mid-level and deep features from the CLIP encoder. It then leverages robust deep features through a semantically guided cross-attention mechanism to filter and select detail-rich shallow features, followed by further feature fusion learning through a self-attention block. This process generates a category-independent visual refinement representation, which is then mapped to a category-specific residual refinement map via text embedding. Finally, the learned refined map is fused with the original coarse affinity map of CLIP through simple element-wise addition to obtain the final segmentation result.

We train our ARM once on the COCO-Stuff [24] dataset and deploy it as a fixed, plug-and-play post-processor across some training-free OVSS frameworks. Extensive experiments on standard benchmarks validate our approach.

Our main contributions are summarized as follows:

- We propose the Attention Refinement Module (ARM), a lightweight, trainable module that learns to refine hierarchical features to improve CLIP’s pixel-level predictions. We demonstrate its superiority over other methods, establishing a more effective path for mining VLMs internal potential.
- We validate the generality and plug-and-play capability of ARM. Trained once, it exhibits strong zero-shot transferability, consistently boosting diverse training-free models on multiple unseen datasets.
- Our work reveals the significant, untapped learnable potential within CLIP’s internal features, offering a new, efficient paradigm for OVSS that moves beyond static heuristics and reliance on costly external foundation models.

## 2 Related Work

Research in Open-Vocabulary Semantic Segmentation (OVSS), catalyzed by the advent of CLIP [1], has bifurcated into two principal paradigms: training-based and training-free methods. We review both, with a focus on the latter, to which our work belongs.

**Training-Based Methods.** These methods fine-tune the VLM or introduce learnable components to adapt CLIP for dense prediction tasks. Pioneering works like LSeg [25] and OVSeg [3] align CLIP embeddings with pixel-level features from a segmentation backbone. ZegFormer [26] employs a transformer decoder for zero-shot generalization, while SAN [8] introduces side adapters to efficiently fine-tune frozen backbones. ODISE [27] leverages diffusion models for panoptic mask generation, and TCL [28] focuses on text-conditioned learning. Other notable approaches include CLIPSeg [29], which adds a segmentation head to CLIP; DenseCLIP [30], emphasizing dense feature alignment; SegCLIP [6], pre-training on synthetic data;

and FC-CLIP [31], fusing features across scales. GroupViT [32] groups visual tokens for hierarchical segmentation, and CRIS [33] uses contrastive learning for region-text alignment. While effective on some benchmarks, these methods may risk overfitting to seen classes and compromising the VLM’s inherent zero-shot capabilities [2], often requiring substantial computational resources for training.

**Training-Free Methods.** To preserve zero-shot generalization, these methods avoid fine-tuning the VLM, instead post-processing its outputs with auxiliary cues. Gaining traction for their efficiency, early efforts [2, 34] were the first to expose CLIP’s localization limits from image-level training. Recent works mitigate this via two strategies: reliance on external foundation models or mining internal CLIP potentials.

**Training-Free Refinement via External Models.** A prevalent approach compensates for CLIP’s coarse localization by importing spatial priors from external vision foundation models (VFM) like SAM [18], DINO/DINOv2 [19, 20], or Stable Diffusion (SD) [21]. For example, PerSAM [35] personalizes SAM with CLIP prompts. CorrCLIP [15] uses SAM masks for scope reconstruction and DINO features for value reconstruction to suppress inter-class correlations. CLIPer [14] employs SD for fine-grained compensation alongside internal attention fusion. FreeSeg [36] generates free-form masks via SD inpainting guided by CLIP. ReCo [37] uses retrieval-augmented contrast for external knowledge integration. ZegCLIP [10] incorporates external detectors for proposal generation. However, these methods introduce dependencies on multiple large models, increasing computational overhead and complicating inference pipelines.

**Training-Free Refinement via Internal Potential.** An alternative, more lightweight paradigm unlocks localization cues from within the frozen CLIP model, avoiding external dependencies. This line of work diagnoses issues in CLIP’s Vision Transformer (ViT) [22], where deep layers exhibit spatially-invariant attention [19, 23]. Methods evolve along two paths.

*Self-Attention Modification.* These approaches heuristically modify the final-layer attention to restore localization. GEM [38] proposes a method to compute the attention matrix by combining query-query, query-key, and value-value attention. SCLIP [11] replaces query-key self-attention with query-query and key-key mechanisms. ClearCLIP [5] removes noisy residuals and feedforward neural networks in the last layer. CLIPtrase [39] attempts to cluster global image patches for segmentation using a weighted average of autocorrelation attention mechanisms. NAACLIP [12] incorporates neighboring priors into key-key attention. AttCLIP [40] enhances attention with adaptive gating. CLIP-Surgery [41] surgically corrects attention patterns by analyzing and removing noisy keys and residuals.

*Fusion of Intermediate Cues.* Recognizing valuable signals in intermediate ViT layers [23], these methods attempt to aggregate them. ResCLIP [4] averages intermediate maps as residuals to correct final-layer outputs. CLIPer’s early-layer

fusion [14] statically averages attention maps to replace the final one. While validating the utility of intermediate cues, these methods rely on static, hand-crafted fusion strategies (e.g., simple averaging) rather than a learned, adaptive mechanism to fuse these multi-scale features.

We position ARM between static, untrained fusion and fully supervised segmentation. This makes it distinct from both static heuristics and task-specific decoders.

## 3 Methodology

Our core idea is to maximally exploit the features learned intrinsically by CLIP to refine its coarse segmentation, thereby avoiding the dependency on external models. We achieve this by learning a residual refinement signal derived purely from CLIP’s own multi-level features. The overall pipeline, illustrated in Figure 2, first extracts multi-level features from the CLIP visual encoder. These features are then fed into our proposed Attention Refinement Module (ARM) to generate a refinement map, which is simply fused with the original coarse affinity map in the end.

### 3.1 Preliminary

Our approach builds upon the standard training-free OVSS paradigm. Given an input image  $I \in \mathbb{R}^{H \times W \times 3}$  and a set of text prompts  $\mathcal{T} = \{t_1, \dots, t_C\}$  for  $C$  target classes.

First, we utilize the frozen CLIP text encoder to encode the prompts into text embeddings  $E_t \in \mathbb{R}^{C \times D}$ , where  $D$  is the feature dimension. Simultaneously, the image  $I$  is fed into the frozen CLIP ViT visual encoder. We extract the output from its final transformer block (excluding the [CLS] token) to obtain patch features  $F_d \in \mathbb{R}^{N \times D}$ , where  $N = (H/P) \times (W/P)$  is the number of patches and  $P$  is the patch size.

Following [1], we generate the coarse affinity map by computing the normalized cosine similarity between  $F_d$  and  $E_t$ , scaled by the learnable temperature coefficient  $\tau$ :

$$S_c = \text{Softmax}(\tau \cdot \frac{F_d}{\|F_d\|} \cdot \frac{E_t^\top}{\|E_t\|}) \quad (1)$$

This affinity map  $S_c \in \mathbb{R}^{N \times C}$  provides the basic semantic localization for the target classes, but it suffers from low spatial resolution and lacks fine-grained boundary details. We reshape and upsample it to  $M_c \in \mathbb{R}^{C \times H' \times W'}$  to serve as the baseline for subsequent refinement.

### 3.2 Attention Refinement Module

To overcome the spatial coarseness of  $M_c$ , we designed an Attention Refinement Module (ARM), which is lightweight and transferable to other training-free methods. The core principle of this module is to perform “self-correction” by

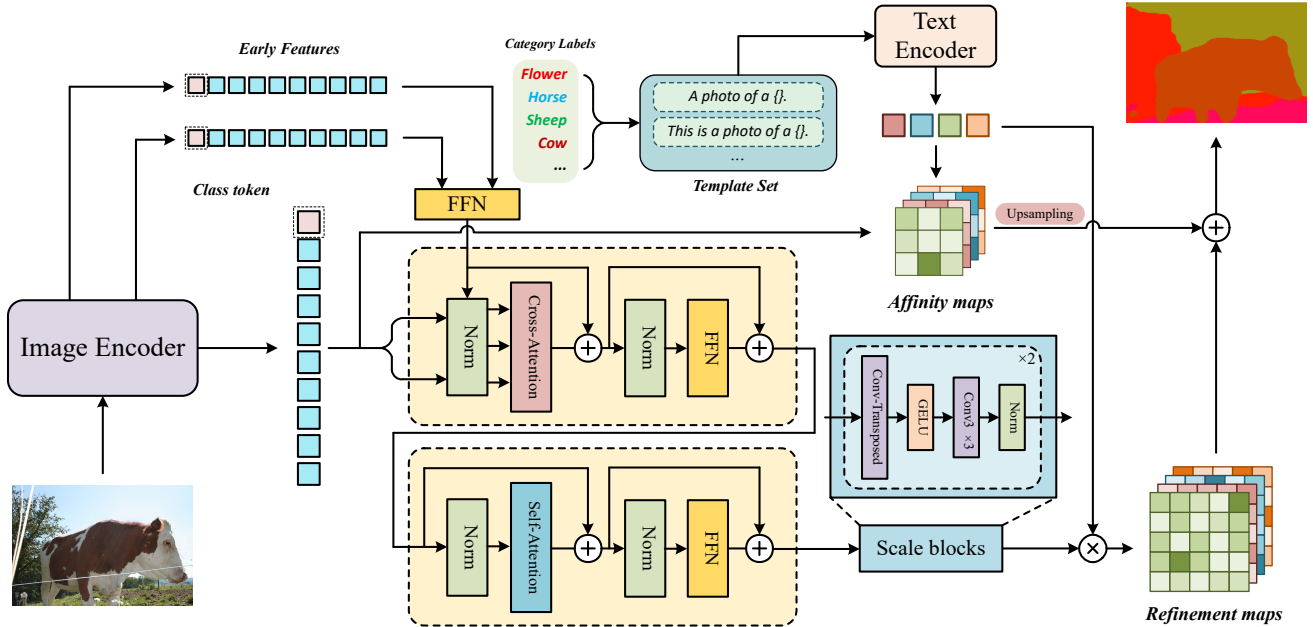


Figure 2: Our Attention Refinement Module (ARM) architecture. ARM extracts hierarchical features from the image encoder and fuses them sequentially through cross-attention and self-attention mechanisms. The fused features are processed by Scale blocks to generate a class-agnostic affinity map. This map is then multiplied by the text embedding ( $\otimes$ ) to generate a class-related refined map. Finally, this refined map is added ( $\oplus$ ) to the original coarse affinity map to correct localization errors and restore details.

leveraging features from different hierarchical levels within CLIP.

As [14] and [4] suggested that CLIP’s shallow and mid-level features contain the low-level edge and texture information that is often smoothed out in the final features. We modify the forward pass of the CLIP vision encoder to extract intermediate patch features from ViT layers  $l_i$  and  $l_j$  (e.g., 3rd layer and 7th layer). These features are concatenated and projected through a small MLP to obtain  $F_m \in \mathbb{R}^{N \times D}$  with a unified dimension, aligning it with  $F_d$ . The ARM takes both  $F_m$  and  $F_d$  as input, and its internal structure involves two key steps.

**Semantic-guided Cross-Attention.** We first use  $F_m$  as the query and  $F_d$  as the key and value, fusing them through a stack of cross-attention blocks. This is formulated as follows:

$$\begin{aligned} F'_m &= \text{Cross-Attn}(F_m, F_d, F_d) \\ &= \text{Softmax}\left(\frac{F_m \cdot F_d^\top}{\sqrt{d}}\right) \cdot F_d \end{aligned} \quad (2)$$

where  $d$  is the dimensionality of the keys. This step uses the robust global semantics of  $F_d$  to guide and filter the low-level details in  $F_m$ , focusing them on semantically relevant edges and textures.

**Spatial Consistency Self-Attention.** The fused feature  $F'_m$  is then passed through a stack of self-attention blocks to

enhance internal spatial consistency and contextual awareness:

$$\begin{aligned} F''_m &= \text{Self-Attn}(F'_m, F'_m, F'_m) \\ &= \text{Softmax}\left(\frac{F'_m \cdot F'^\top}{\sqrt{d}}\right) \cdot F'_m \end{aligned} \quad (3)$$

After attention fusion, the resulting  $F''_m$  is fed into a lightweight Scale Block (see Figure 2). This module consists of transposed convolutions, which are mainly responsible for upsampling the features while restoring some spatial details of the current features. This process generates a class-independent visual representation  $R_v \in \mathbb{R}^{D \times H' \times W'}$ .

Finally, we project  $R_v$  into a class-specific refinement map  $M_r \in \mathbb{R}^{C \times H' \times W'}$  using the text embeddings  $E_t$ :

$$M_r = E_t \cdot R_v \quad (4)$$

$M_r$  will be the correctional signal for  $M_c$ , concentrating on boundaries and easily confused regions.

To combine the coarse global semantics from  $M_c$  with the fine-grained local corrections from  $M_r$  and minimize the impact on the original model, we simply fuse them using simple element-wise addition to get an initial fused map  $M_f$ :

$$M_f = M_c + M_r \quad (5)$$

This residual connection allows the refinement module to focus on learning the correction signal rather than reconstructing the entire segmentation map from scratch.

## 4 Experiments

### 4.1 Experimental Setups

**Datasets.** We train our ARM once on the COCO-Stuff (Stuff) [24]. For zero-shot evaluation, we use five standard benchmarks: PASCAL VOC 2012 (VOC-20/21) [42], PASCAL Context (Context-59/60) [43], ADE20K (ADE-150) [44]. And in Section 4.3, we also used the COCO-Object (Object) [24] dataset for ablation. We compare all the semantic segmentation results using mean Intersection over Union (mIoU).

**Architecture.** Our experiments primarily use the CLIP ViT-B/16 backbone, with additional results provided for ViT-L/14. The CLIP model itself remains frozen during both ARM training and inference. By default, our ARM extracts intermediate features from 3rd layer and 7th layer, comprising one cross-attention block and one self-attention block.

**Training details.** We train only the ARM using the Binary Cross-Entropy (BCE) loss on COCO-Stuff [24] for 5 epochs. We use the AdamW [45] optimizer with a learning rate of  $1 \times 10^{-4}$ , a batch size of 4, and a weight decay of  $1 \times 10^{-3}$ .

**Inference.** During evaluation, the trained ARM is frozen and applied as a post-processor to the baseline affinity map.

### 4.2 Main Results

Initially, we trained the ARM using the original CLIP [1], and the results were acceptable. However, when transferring it to other training-free methods, performance dropped noticeably. We noticed that most current training-free methods use a Clear-CLIP [5] configuration, such as removing the residual connections and feedforward neural networks in the last layer. Therefore, we first trained the ARM under the Clear-CLIP configuration and then transferred it to CLIPer, achieving better performance, as shown in Figure 3.

**Reference comparison with training-based methods.** To position our method within the broader OVSS landscape, we first present a reference comparison in Table 1 between our ARM (applied to the ClearCLIP baseline) and current mainstream training-based methods.

We first wish to clarify a significant paradigm disparity: These training-based methods are fully end-to-end trained architectures that are deeply optimized for the segmentation task. In contrast, our ARM is a lightweight plug-and-play module designed with a greater emphasis on maintaining generality and efficiency. This difference in training paradigms is predictably reflected in performance. As expected, in dense scenarios like ADE-150 and Context-459, the training-based models exhibit a significant performance ceiling. We believe this gap is reasonable due to the complexity and specialization of the models.

**Quantitative results of ARM in zero-shot transfer.** Table 2 illustrates the zero-shot transfer capability of ARM as a plug-and-play module. Our ARM delivers significant mIoU gains

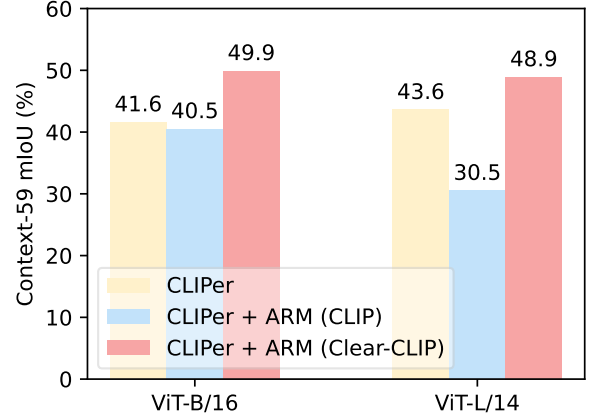


Figure 3: Zero-shot transfer results of applying ARM to CLIPer on the Context-59. The ARM trained with standard CLIP features (blue) resulted in a performance degradation, while the ARM trained with Clear-CLIP features (red) resulted in a significant performance improvement.

for all baseline methods. For the ViT-B/16 architecture, ARM improves the average mIoU of SCLIP from 44.8% to 53.7% and CLIPer from 50.4% to 55.0%. This improvement is equally robust on the ViT-L/14 architecture. This demonstrates the potential of ARM as a general-purpose post-processing module.

Additionally, the introduction of ARM results in a slight performance degradation of the model on the ADE-150 dataset. We attribute this to the inherent complexity of the ADE-150 dataset, which places exceptionally high demands on a model’s feature extraction capabilities. In contrast, our ARM is designed with a lightweight and concise architecture. This compact design may limit its capacity to learn the rich features required for fine-grained segmentation in such complex scenarios. Consequently, the refinement map generated by ARM may conflict with or interfere with the segmentation results of baseline models, leading to a slight performance degradation. Despite the limitations mentioned above, our method achieved a competitive level in the remaining benchmarks.

**Qualitative results.** As shown in Figure 4, these examples demonstrate that our method offers some visual improvements. For instance, while CLIPer’s output captures the general global semantics, it has limitations in capturing object boundaries and fine textures. When zero-shot transfer is applied to our ARM, the baseline model’s performance in these areas is significantly improved; boundary regions appear clearer, with reduced background noise. In contrast, while ResCLIP also attempts to utilize intermediate features, its static fusion strategy and the subsequent PAMR [47] post-processing appear to introduce artifacts or lose details in certain situations.

This suggests that ARM, as a general, learnable refinement module, with its adaptive feature extraction paradigm, may

Table 1: Reference Comparison with Training-Based Methods. We provide this comparison to contextualize the performance of our lightweight, ‘train-once’ module against fully-trained methods.

Method	Backbone	Training Set	Context-459	Context-59	VOC-20	ADE-150	VOC-21
TCL [28]	ViT-B/16	CC-12M	-	33.9	83.2	17.1	55.0
OVSeg [3]	ViT-B/16	COCO-Stuff	11.0	53.3	92.6	24.8	-
CAT-Seg [7]	ViT-B/16	COCO-Stuff	19.0	57.5	94.6	31.8	77.3
SAN [8]	ViT-B/16	COCO-Stuff	12.6	53.8	94.0	27.5	-
SED [9]	ConvNeXt-B	COCO-Stuff	18.6	57.3	94.4	31.6	-
ESC-Net [46]	ViT-B/16	COCO-Stuff	21.1	59.0	97.3	35.6	80.1
<b>ARM-CLIP (Ours)</b>	ViT-B/16	COCO-Stuff	9.6	49.9	89.3	17.8	73.3
OVSeg [3]	ViT-L/14	COCO-Stuff	11.0	53.3	92.6	24.8	-
CAT-Seg [7]	ViT-L/14	COCO-Stuff	19.0	57.5	94.6	31.8	82.5
SAN [8]	ViT-L/14	COCO-Stuff	12.6	53.8	94.0	27.5	-
SED [9]	ConvNeXt-L	COCO-Stuff	18.6	57.3	94.4	31.6	-
ESC-Net [46]	ViT-L/14	COCO-Stuff	21.1	59.0	97.3	35.6	86.3
<b>ARM-CLIP (Ours)</b>	ViT-L/14	COCO-Stuff	10.6	50.9	92.6	18.7	69.3

Table 2: Performance comparison with training-free state-of-the-art methods. We apply the trained ARM to training-free methods using zero-shot transfer. Note that the ARM is trained using the Clear-CLIP setup.

Method	Backbone	Context-60	Context-59	VOC-20	ADE-150	VOC-21	Average
CLIP [1]	ViT-B/16	8.4	9.2	41.9	2.9	16.4	15.8
MaskCLIP [2]	ViT-B/16	23.6	26.4	74.9	9.8	38.8	34.7
ClearCLIP [5]	ViT-B/16	32.6	35.9	80.9	17.7	51.8	43.8
NACLIP [12]	ViT-B/16	35.0	38.4	83.0	19.1	64.1	47.9
CorrCLIP [15]	ViT-B/16	44.2	48.8	88.8	<b>26.9</b>	<b>74.8</b>	<b>56.7</b>
ResCLIP [4]	ViT-B/16	33.5	36.8	86.0	18.0	61.1	47.0
SCLIP [11]	ViT-B/16	34.2	34.2	80.4	16.1	59.1	44.8
CLIPer [14]	ViT-B/16	37.6	41.7	85.2	<u>21.4</u>	65.9	50.4
<b>SCLIP + ARM</b>	ViT-B/16	<u>45.3</u>	48.1	88.5	17.1	69.5	<b>53.7 (+8.9)</b>
<b>CLIPer + ARM</b>	ViT-B/16	<b>45.6</b>	<b>49.5</b>	<b>89.3</b>	17.5	<u>73.2</u>	<u>55.0 (+4.6)</u>
CLIP [1]	ViT-L/14	4.1	4.4	15.6	1.7	8.2	6.8
MaskCLIP [2]	ViT-L/14	11.7	12.4	29.4	7.2	23.3	16.8
ClearCLIP [5]	ViT-L/14	26.7	29.6	80.0	15.0	46.1	39.5
CorrCLIP [15]	ViT-L/14	<u>44.9</u>	<b>50.8</b>	<u>91.5</u>	<b>30.7</b>	<b>76.7</b>	<b>58.9</b>
ResCLIP [4]	ViT-L/14	30.9	34.5	85.5	18.2	54.1	44.6
SCLIP [11]	ViT-L/14	22.3	25.2	69.1	10.9	43.5	34.2
CLIPer [14]	ViT-L/14	38.0	43.6	90.0	<u>24.4</u>	69.8	53.2
<b>SCLIP + ARM</b>	ViT-L/14	42.9	46.9	89.8	17.5	65.8	<b>52.6 (+18.4)</b>
<b>CLIPer + ARM</b>	ViT-L/14	<b>46.3</b>	<u>50.7</u>	<b>92.5</b>	18.2	<u>71.6</u>	<u>55.9 (+2.7)</u>

offer a valuable supplement to improving the detail performance of baseline models compared to static fusion strategies, demonstrating its effectiveness and potential.

**Efficiency Analysis.** Table 3 shows that our ARM adds minimal computational overhead while delivering substantial mIoU improvements. This positions our method as a highly efficient alternative to external model fusion and a more performant option compared to static internal fusion methods like

ResCLIP.

### 4.3 Ablation Studies

All ablation experiments were performed by transferring our trained ARM to the CLIPer architecture, and were evaluated on Context-59 using ViT-B/16 as the backbone, unless otherwise specified. Our goal was to validate key design choices in the

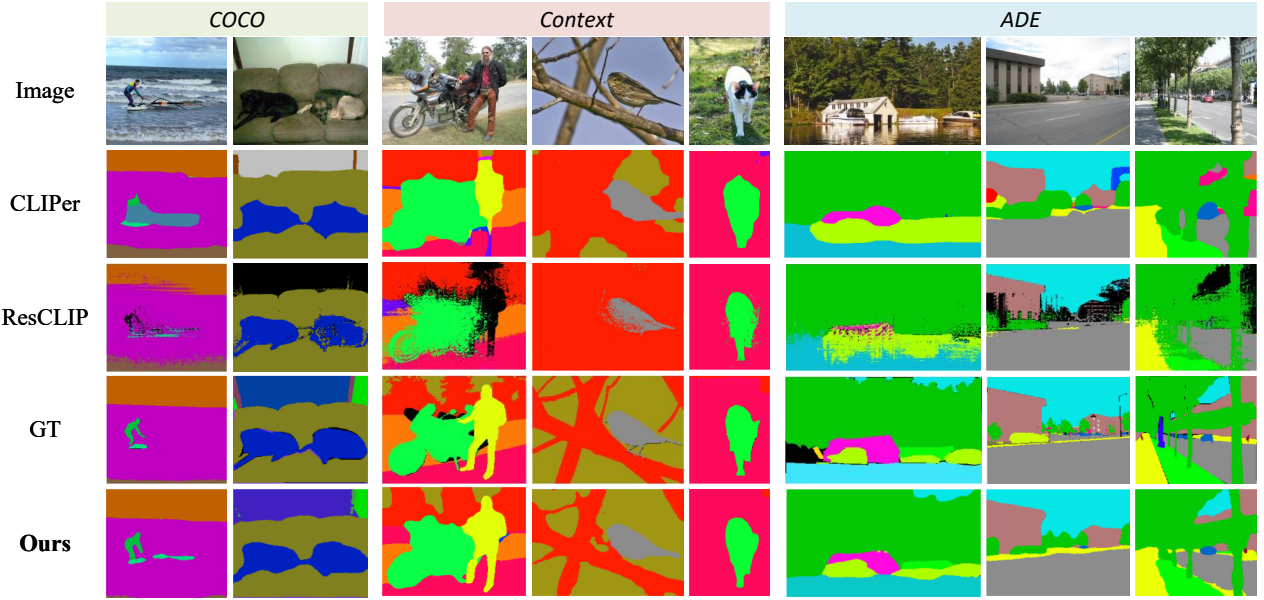


Figure 4: **Qualitative Results.** Visual comparison on sample images from three different datasets. Compared to these methods, our method has more accurate segmentation results that are closer to the ground-truths.

Table 3: Efficiency in reporting the average inference time per image on a single NVIDIA Tesla V100 GPU.

Method	Backbone	Time (ms)	Context-59
NACLIP	ViT-B/16	84.2	35.2
ResCLIP	ViT-B/16	64.5	36.8
CLIPer	ViT-B/16	35.4	41.7
<b>Ours</b>	ViT-B/16	<b>53.2 (+20.8)</b>	<b>49.5 (+8.8)</b>
NACLIP	ViT-L/14	101.9	32.1
ResCLIP	ViT-L/14	80.8	34.5
CLIPer	ViT-L/14	67.8	43.6
<b>Ours</b>	ViT-L/14	<b>79.7 (+11.9)</b>	<b>50.8 (+7.2)</b>

Table 4: Ablation on intermediate layer selection.

Fusion Layers	Context-59	ADE-150	Object
(1st, 3rd)	45.2	15.2	55.3
(1st, 5th)	47.9	16.8	59.4
(1st, 7th)	48.2	17.0	61.8
(3rd, 5th)	47.9	16.5	59.5
<b>(3rd, 7th)</b>	<b>49.5</b>	<b>17.5</b>	<b>63.5</b>
(5th, 7th)	48.6	16.9	62.6

ARM.

**Choice of Intermediate Layers.** We first investigate the impact of fusing features from different depths of the ViT backbone. Generally, fusing features from different levels

usually yields better results, and our data also demonstrates this, as shown in Table 4. For example, using the feature maps of the 1st layer and 3rd layer results in a lack of semantic features, ultimately achieving mIoU of 45.2%, 15.2%, and 55.3% on the Context-59, ADE-150, and Object datasets, respectively. However, Combining a shallow layer, which may preserve more spatial details, with a deep layer containing richer semantic context yields optimal performance. As the experimental results show, using features from the 3rd layer and 7th layer yields better results.

Table 5: Ablation on the number of self-attention and cross-attention layers.

Number of attention layers	Context-59	Object
(0, 0)	42.2	51.8
(0, 1)	43.1	53.5
(1, 0)	45.7	55.2
<b>(1, 1)</b>	<b>49.5</b>	<b>63.5</b>
(2, 1)	49.1	62.1
(1, 2)	49.5	62.3
(2, 2)	49.4	63.2

**ARM Component Analysis.** Table 5 shows the contribution of self-attention and cross-attention in ARM.  $(x, y)$  means there are  $x$  self-attention layers and  $y$  cross-attention layers. We observed that stacking more layers did not yield further gains and slightly reduced performance. As shown in Table 5, increasing the number of layers from  $(1, 1)$  to  $(2, 1)$ ,  $(1, 2)$ , or

Table 6: Ablation on both attention layers and Scale Blocks.

Number of attention layers	Scale blocks	Context-59
(0, 0)	✗	40.1
(0, 0)	✗	42.2
(1, 1)	✗	46.6
<b>(1, 1)</b>	<b>✓</b>	<b>49.5</b>

(2, 2) resulted in almost no change in the mIoU score, or only a very slight decrease. This indicates that simply increasing the module depth does not provide additional performance gains. Given that increasing the number of layers incurs additional parameters and computational costs without a corresponding performance return, we therefore selected (1, 1) as the optimal configuration, which aligns with our goal to design efficient and lightweight modules.

We also validate the contribution of Scale Blocks in Table 6. Removing both the attention module and the scale blocks results in a baseline of 40.1% mIoU. Adding just the scale blocks provides a modest improvement by 2.1% mIoU. Using only the attention module without scale blocks brings a substantial gain to 46.6% mIoU, demonstrating it is the core of the refinement. Finally, combining both the attention module and the scale blocks achieves our best performance. This suggests that while the attention mechanism performs the primary feature refinement, the learnable upsampling blocks are also beneficial for generating the final high-quality refinement map.

## 5 Conclusion

In this paper, we propose ARM, a lightweight, learnable, plug-and-play module. ARM learns how to adaptively fuse hierarchical features within CLIP, leveraging the robust semantics of deep features to guide and filter detail-rich shallow features. The core innovation lies in the “train once, use everywhere” paradigm. ARM, trained once on a benchmark dataset, can serve as a general-purpose post-processor, enabling zero-shot transfer to various training-independent frameworks. More importantly, the inference overhead resulting from this performance improvement is negligible. Our work highlights the learnable potential inherent in CLIP’s internal features, and explores a practical paradigm for lightweight, training-free open-vocabulary segmentation.

## References

- [1] Alec Radford, Jong Wook Kim, Chris Hallacy, Aditya Ramesh, Gabriel Goh, Sandhini Agarwal, Girish Sastry, Amanda Askell, Pamela Mishkin, Jack Clark, Gretchen Krueger, and Ilya Sutskever. Learning transferable visual models from natural language supervision, 2021.
- [2] Xiaoyi Dong, Jianmin Bao, Yinglin Zheng, Ting Zhang, Dong-  
dong Chen, Hao Yang, Ming Zeng, Weiming Zhang, Lu Yuan, Dong Chen, et al. Maskclip: Masked self-distillation advances contrastive language-image pretraining. In *Proceedings of the IEEE/CVF conference on computer vision and pattern recognition*, pages 10995–11005, 2023.
- [3] Feng Liang, Bichen Wu, Xiaoliang Dai, Kunpeng Li, Yinan Zhao, Hang Zhang, Peizhao Zhang, Peter Vajda, and Diana Marculescu. Open-vocabulary semantic segmentation with mask-adapted clip. In *Proceedings of the IEEE/CVF conference on computer vision and pattern recognition*, pages 7061–7070, 2023.
- [4] Yuhang Yang, Jinhong Deng, Wen Li, and Lixin Duan. Resclip: Residual attention for training-free dense vision-language inference. In *Proceedings of the Computer Vision and Pattern Recognition Conference*, pages 29968–29978, 2025.
- [5] Mengcheng Lan, Chaofeng Chen, Yiping Ke, Xinjiang Wang, Litong Feng, and Wayne Zhang. Clearclip: Decomposing clip representations for dense vision-language inference. In *European Conference on Computer Vision*, pages 143–160. Springer, 2024.
- [6] Huaishao Luo, Junwei Bao, Youzheng Wu, Xiaodong He, and Tianrui Li. Segclip: Patch aggregation with learnable centers for open-vocabulary semantic segmentation. In *International Conference on Machine Learning*, pages 23033–23044. PMLR, 2023.
- [7] Seokju Cho, Heeseong Shin, Sunghwan Hong, Anurag Arnab, Paul Hongseok Seo, and Seungryong Kim. Cat-seg: Cost aggregation for open-vocabulary semantic segmentation. In *Proceedings of the IEEE/CVF Conference on Computer Vision and Pattern Recognition*, pages 4113–4123, 2024.
- [8] Mengde Xu, Zheng Zhang, Fangyun Wei, Han Hu, and Xiang Bai. Side adapter network for open-vocabulary semantic segmentation. In *Proceedings of the IEEE/CVF conference on computer vision and pattern recognition*, pages 2945–2954, 2023.
- [9] Bin Xie, Jiale Cao, Jin Xie, Fahad Shahbaz Khan, and Yanwei Pang. Sed: A simple encoder-decoder for open-vocabulary semantic segmentation. In *Proceedings of the IEEE/CVF conference on computer vision and pattern recognition*, pages 3426–3436, 2024.
- [10] Ziqin Zhou, Yinjie Lei, Bowen Zhang, Lingqiao Liu, and Yifan Liu. Zegclip: Towards adapting clip for zero-shot semantic segmentation. In *Proceedings of the IEEE/CVF conference on computer vision and pattern recognition*, pages 11175–11185, 2023.
- [11] Feng Wang, Jieru Mei, and Alan Yuille. Sclip: Rethinking self-attention for dense vision-language inference. In *European Conference on Computer Vision*, pages 315–332. Springer, 2024.
- [12] Sina Hajimiri, Ismail Ben Ayed, and Jose Dolz. Pay attention to your neighbours: Training-free open-vocabulary semantic segmentation. In *2025 IEEE/CVF Winter Conference on Applications of Computer Vision (WACV)*, pages 5061–5071. IEEE, 2025.

[13] Mengcheng Lan, Chaofeng Chen, Yiping Ke, Xinjiang Wang, Litong Feng, and Wayne Zhang. Proxyclip: Proxy attention improves clip for open-vocabulary segmentation. In *European Conference on Computer Vision*, pages 70–88. Springer, 2024.

[14] Lin Sun, Jiale Cao, Jin Xie, Xiaoheng Jiang, and Yanwei Pang. Cliper: Hierarchically improving spatial representation of clip for open-vocabulary semantic segmentation. In *Proceedings of the IEEE/CVF International Conference on Computer Vision*, pages 23199–23209, 2025.

[15] Dengke Zhang, Fagui Liu, and Quan Tang. Corrclip: Reconstructing patch correlations in clip for open-vocabulary semantic segmentation. In *Proceedings of the IEEE/CVF International Conference on Computer Vision*, pages 24677–24687, 2025.

[16] Vladan Stojnić, Yannis Kalantidis, Jiří Matas, and Giorgos Tolias. Lposs: Label propagation over patches and pixels for open-vocabulary semantic segmentation. In *Proceedings of the Computer Vision and Pattern Recognition Conference*, pages 9794–9803, 2025.

[17] Monika Wysoczańska, Oriane Siméoni, Michaël Ramamonjisoa, Andrei Bursuc, Tomasz Trzcinski, and Patrick Pérez. Clip-dinoiser: Teaching clip a few dino tricks for open-vocabulary semantic segmentation. *ECCV*, 2024.

[18] Alexander Kirillov, Eric Mintun, Nikhila Ravi, Hanzi Mao, Chloe Rolland, Laura Gustafson, Tete Xiao, Spencer Whitehead, Alexander C Berg, Wan-Yen Lo, et al. Segment anything. In *Proceedings of the IEEE/CVF international conference on computer vision*, pages 4015–4026, 2023.

[19] Mathilde Caron, Hugo Touvron, Ishan Misra, Hervé Jégou, Julien Mairal, Piotr Bojanowski, and Armand Joulin. Emerging properties in self-supervised vision transformers. In *Proceedings of the IEEE/CVF international conference on computer vision*, pages 9650–9660, 2021.

[20] Maxime Oquab, Timothée Darcet, Théo Moutakanni, Huy Vo, Marc Szafraniec, Vasil Khalidov, Pierre Fernandez, Daniel Haziza, Francisco Massa, Alaeldin El-Nouby, et al. Dinov2: Learning robust visual features without supervision. *arXiv preprint arXiv:2304.07193*, 2023.

[21] Robin Rombach, Andreas Blattmann, Dominik Lorenz, Patrick Esser, and Björn Ommer. High-resolution image synthesis with latent diffusion models. In *Proceedings of the IEEE/CVF conference on computer vision and pattern recognition*, pages 10684–10695, 2022.

[22] Alexey Dosovitskiy. An image is worth 16x16 words: Transformers for image recognition at scale. *arXiv preprint arXiv:2010.11929*, 2020.

[23] Maithra Raghu, Thomas Unterthiner, Simon Kornblith, Chiyuan Zhang, and Alexey Dosovitskiy. Do vision transformers see like convolutional neural networks? *Advances in neural information processing systems*, 34:12116–12128, 2021.

[24] Holger Caesar, Jasper Uijlings, and Vittorio Ferrari. Coco-stuff: Thing and stuff classes in context. In *Proceedings of the IEEE conference on computer vision and pattern recognition*, pages 1209–1218, 2018.

[25] Boyi Li, Kilian Q Weinberger, Serge Belongie, Vladlen Koltun, and Rene Ranftl. Language-driven semantic segmentation. In *International Conference on Learning Representations*, 2022.

[26] Jian Ding, Nan Xue, Gui-Song Xia, and Dengxin Dai. Decoupling zero-shot semantic segmentation. In *Proceedings of the IEEE/CVF conference on computer vision and pattern recognition*, pages 11583–11592, 2022.

[27] Jiarui Xu, Sifei Liu, Arash Vahdat, Wonmin Byeon, Xiaolong Wang, and Shalini De Mello. Open-vocabulary panoptic segmentation with text-to-image diffusion models. In *Proceedings of the IEEE/CVF conference on computer vision and pattern recognition*, pages 2955–2966, 2023.

[28] Junbum Cha, Jonghwan Mun, and Byungseok Roh. Learning to generate text-grounded mask for open-world semantic segmentation from only image-text pairs. In *Proceedings of the IEEE/CVF Conference on Computer Vision and Pattern Recognition (CVPR)*, 2023.

[29] Timo Lüddecke and Alexander Ecker. Image segmentation using text and image prompts. In *Proceedings of the IEEE/CVF conference on computer vision and pattern recognition*, pages 7086–7096, 2022.

[30] Yongming Rao, Wenliang Zhao, Guangyi Chen, Yansong Tang, Zheng Zhu, Guan Huang, Jie Zhou, and Jiwen Lu. Denseclip: Language-guided dense prediction with context-aware prompting. In *Proceedings of the IEEE/CVF conference on computer vision and pattern recognition*, pages 18082–18091, 2022.

[31] Qihang Yu, Ju He, Xueqing Deng, Xiaohui Shen, and Liang-Chieh Chen. Convolutions die hard: Open-vocabulary segmentation with single frozen convolutional clip. *Advances in Neural Information Processing Systems*, 36:32215–32234, 2023.

[32] Jiarui Xu, Shalini De Mello, Sifei Liu, Wonmin Byeon, Thomas Breuel, Jan Kautz, and Xiaolong Wang. Groupvit: Semantic segmentation emerges from text supervision. In *Proceedings of the IEEE/CVF conference on computer vision and pattern recognition*, pages 18134–18144, 2022.

[33] Zhaoqing Wang, Yu Lu, Qiang Li, Xunqiang Tao, Yandong Guo, Mingming Gong, and Tongliang Liu. Cris: Clip-driven referring image segmentation. In *Proceedings of the IEEE/CVF conference on computer vision and pattern recognition*, pages 11686–11695, 2022.

[34] Mengde Xu, Zheng Zhang, Fangyun Wei, Yutong Lin, Yue Cao, Han Hu, and Xiang Bai. A simple baseline for open-vocabulary semantic segmentation with pre-trained vision-language model. In *European Conference on Computer Vision*, pages 736–753. Springer, 2022.

[35] Renrui Zhang, Zhengkai Jiang, Ziyu Guo, Shilin Yan, Junting Pan, Hao Dong, Peng Gao, and Hongsheng Li. Personalize segment anything model with one shot. *arXiv preprint arXiv:2305.03048*, 2023.

[36] Jie Qin, Jie Wu, Pengxiang Yan, Ming Li, Ren Yuxi, Xuefeng Xiao, Yitong Wang, Rui Wang, Shilei Wen, Xin Pan, et al. Freeseg: Unified, universal and open-vocabulary image segmentation. In *Proceedings of the IEEE/CVF Conference on Computer Vision and Pattern Recognition*, pages 19446–19455, 2023.

[37] Gyungin Shin, Weidi Xie, and Samuel Albanie. Reco: Retrieve and co-segment for zero-shot transfer. *Advances in Neural Information Processing Systems*, 35:33754–33767, 2022.

[38] Walid Bousselham, Felix Petersen, Vittorio Ferrari, and Hilde Kuehne. Grounding everything: Emerging localization properties in vision-language transformers. In *Proceedings of the IEEE/CVF Conference on Computer Vision and Pattern Recognition*, pages 3828–3837, 2024.

[39] Tong Shao, Zhuotao Tian, Hang Zhao, and Jingyong Su. Explore the potential of clip for training-free open vocabulary semantic segmentation. In *European Conference on Computer Vision*, pages 139–156. Springer, 2024.

[40] Tong Shao, Zhuotao Tian, Hang Zhao, and Jingyong Su. Explore the potential of clip for training-free open vocabulary semantic segmentation. In *European Conference on Computer Vision*, pages 139–156. Springer, 2024.

[41] Yi Li, Hualiang Wang, Yiqun Duan, Jiheng Zhang, and Xiaomeng Li. A closer look at the explainability of contrastive language-image pre-training. *Pattern Recognition*, 162:111409, 2025.

[42] Mark Everingham, SM Ali Eslami, Luc Van Gool, Christopher KI Williams, John Winn, and Andrew Zisserman. The pascal visual object classes challenge: A retrospective. *International journal of computer vision*, 111(1):98–136, 2015.

[43] Roozbeh Mottaghi, Xianjie Chen, Xiaobai Liu, Nam-Gyu Cho, Seong-Whan Lee, Sanja Fidler, Raquel Urtasun, and Alan Yuille. The role of context for object detection and semantic segmentation in the wild. In *Proceedings of the IEEE conference on computer vision and pattern recognition*, pages 891–898, 2014.

[44] Bolei Zhou, Hang Zhao, Xavier Puig, Tete Xiao, Sanja Fidler, Adela Barriuso, and Antonio Torralba. Semantic understanding of scenes through the ade20k dataset. *International Journal of Computer Vision*, 127(3):302–321, 2019.

[45] Ilya Loshchilov and Frank Hutter. Decoupled weight decay regularization. *arXiv preprint arXiv:1711.05101*, 2017.

[46] Minhyeok Lee, Suhwan Cho, Jungho Lee, Sunghun Yang, Heeseung Choi, Ig-Jae Kim, and Sangyoun Lee. Effective sam combination for open-vocabulary semantic segmentation. In *Proceedings of the Computer Vision and Pattern Recognition Conference*, pages 26081–26090, 2025.

[47] Nikita Araslanov and Stefan Roth. Single-stage semantic segmentation from image labels. In *IEEE/CVF Conference on Computer Vision and Pattern Recognition (CVPR)*, pages 4253–4262, June 2020.